HAL open science

Fast collective oscillations and clustering phenomena in an antiferromagnetic mean-field model

Arthur Vesperini, Roberto Franzosi, Stefano Ruffo, Andrea Trombettoni, Xavier Leoncini

▶ **To cite this version:**

Arthur Vesperini, Roberto Franzosi, Stefano Ruffo, Andrea Trombettoni, Xavier Leoncini. Fast collective oscillations and clustering phenomena in an antiferromagnetic mean-field model. Chaos, Solitons & Fractals, 2021, 153 (2), pp.111487. 10.1016/j.chaos.2021.111487 . hal-03540783

HAL Id: hal-03540783

https://hal.science/hal-03540783v1

Submitted on 5 Jan 2024

HAL is a multi-disciplinary open access archive for the deposit and dissemination of scientific research documents, whether they are published or not. The documents may come from teaching and research institutions in France or abroad, or from public or private research centers.

L'archive ouverte pluridisciplinaire **HAL**, est destinée au dépôt et à la diffusion de documents scientifiques de niveau recherche, publiés ou non, émanant des établissements d'enseignement et de recherche français ou étrangers, des laboratoires publics ou privés.

Distributed under a Creative Commons Attribution - NonCommercial 4.0 International License

Version of Record: https://www.sciencedirect.com/science/article/pii/S0960077921008419
Manuscript_1e5e788fc3b510d5c8253018f480a3b0

Fast collective oscillations and clustering phenomena in an antiferromagnetic mean-field model

Arthur Vesperini[a,b], Roberto Franzosi[c], Stefano Ruffo[d,e], Andrea Trombettoni[f,g,d], Xavier Leoncini[b]

[a] *Dipartimento di Scienze Fisiche, della Terra e dell'Ambiente (DSFTA), University of Siena, Via Roma 56, 53100 Siena, Italy*
[b] *Aix Marseille Univ, Universite de Toulon, CNRS, CPT, Marseille, France*
[c] *QSTAR & CNR — Istituto Nazionale di Ottica, Largo Enrico Fermi 2, I-50125 Firenze, Italy*
[d] *SISSA and INFN, Sezione di Trieste, Via Bonomea 265, I-34136 Trieste, Italy*
[e] *Istituto dei Sistemi Complessi, Consiglio Nazionale delle Ricerche, Via Madonna del Piano 10, 50019 Sesto Fiorentino, Italy*
[f] *Department of Physics, University of Trieste, Strada Costiera 11, I-34151 Trieste, Italy*
[g] *CNR-IOM DEMOCRITOS Simulation Center, I-34136 Trieste, Italy*

Abstract

We study the out-of-equilibrium properties of the antiferromagnetic Hamiltonian Mean-Field model at low energy. In this regime, the Hamiltonian dynamics exhibits the presence of a long-lived metastable state where the rotators are gathered in a bicluster. This state is not predicted by equilibrium statistical mechanics in the microcanonical ensemble. Performing a low kinetic energy approximation, we derive the explicit expression of the magnetization vector as a function of time. We find that the latter displays coherent oscillations, and we show numerically that the probability distribution for its phase is bimodal or quadrimodal. We then look at the individual rotator dynamics as a motion in an external time-dependent potential, given by the magnetization. This dynamics exhibits two distinct time scales, with the fast one associated to the oscillations of the global magnetization vector. Performing an average over the fast oscillations, we derive an expression for the effective force acting on the individual rotator. This force is always bimodal, and determines a low frequency oscillation of the rotators. Our approach leads to a self-consistent theory linking the time-dependence of the magnetization to the motion of the rotators, providing a heuristic explanation for the formation of the bicluster.

1. Introduction

The Hamiltonian Mean Field (HMF) model has raised much attention in the last two decades [1–10]. This simple toy model indeed exhibits a plethora of phenomena going beyond the scope of equilibrium statistical mechanics, as it is typically the case in long-range interacting systems.

Email addresses: `arthur.vesperini@student.unisi.it` (Arthur Vesperini), `roberto.franzosi@ino.it` (Roberto Franzosi), `ruffo@sissa.it` (Stefano Ruffo), `andreatr@sissa.it` (Andrea Trombettoni), `xavier.leoncini@cpt.univ-mrs.fr` (Xavier Leoncini)

© 2021 published by Elsevier. This manuscript is made available under the CC BY NC user license
https://creativecommons.org/licenses/by-nc/4.0/

As an interesting physical interpretation, the HMF model can be seen as the first Fourier mode approximation of sheet models in one-dimension; the antiferromagnetic HMF model corresponds to a charged sheets model, while the ferromagnetic HMF model corresponds to a massive sheets model [2, 11, 12].

The ferromagnetic HMF undergoes a second order phase transition in both the canonical and microcanonical ensembles [1, 13], while, to the best of our knowledge, there exists no equilibrium phase transition in the antiferromagnetic HMF. However, both the ferromagnetic and the antiferromagnetic HMF are known to present a variety of long-lived metastable states, with relaxation times diverging with the size of the system, thus entailing ergodicity breaking [1, 2, 4–6, 14].
More recently, promising generalizations of the HMF model have been proposed, in which some of these interesting features can be preserved. Notably, some of the aforementioned long-lived metastable states have been shown to be robust with respect to the addition of a (small enough) nearest-neighbours coupling to the model. Phase transition phenomena are still observed in this extended framework [5, 13]. Finite-range versions of the HMF model have also been considered [15, 16], as well as extensions with higher dimensional spins [6, 14], and quantum versions [17], still presenting a rich phenomenology, namely the emergence of non-trivial collective behaviours.

Let us introduce the Hamiltonian of the model. We consider an assembly of N planar classical rotators, endowed with a kinetic energy, subjected to an infinite-range "antiferromagnetic" coupling. This system can also be seen as a collisionless plasma in a one-dimensional ring, with an all-to-all repulsive interaction [3]. The Hamiltonian coordinates of the rotators are $\{\theta_j, p_j\}$. The model can be defined through the Hamiltonian

$$\begin{aligned} H &= \sum_{i=1}^{N} \frac{p_i^2}{2} + V(\{\theta_i\}) \ , \\ \text{with } V(\{\theta_i\}) &= \frac{1}{2N} \sum_{i,j=1}^{N} \cos\left(\theta_i - \theta_j\right) = \frac{N\boldsymbol{M}^2}{2} \ , \end{aligned} \tag{1}$$

where $\boldsymbol{M}$ is the magnetization vector per rotator, defined as

$$\boldsymbol{M} = \frac{1}{N} \sum_{j=1}^{N} \begin{pmatrix} \cos\left(\theta_j\right) \\ \sin\left(\theta_j\right) \end{pmatrix} \ . \tag{2}$$

The equations of motions are

$$\dot{p}_j(t) = M_x \sin\left(\theta_j\right) - M_y \cos\left(\theta_j\right) . \tag{3}$$

The potential of this Hamiltonian is self-consistent, a feature characteristic of mean-field models: the magnetization depends on the single rotator dynamics, which in turn depends on the former.

A homogeneous distribution of the angles of the rotators, implying a vanishing magnetization, is expected at equilibrium in both the canonical and the microcanonical ensemble. However, numerical studies have shown that a long-living coherent structure, namely a bicluster, can spontaneously form in the Hamiltonian

dynamics at low energy [2–4, 7, 8]. This long-lived metastable state consists in the gathering of an extensive quantity of rotators on two opposite angles, and is quantified by the norm M_2 of the vector

$$\boldsymbol{M_2} = \frac{1}{N} \sum_{j=1}^{N} \begin{pmatrix} \cos(2\theta_j) \\ \sin(2\theta_j) \end{pmatrix} . \tag{4}$$

The parameter M_2 varies from 0 in the homogeneous state, to 1 in a bicluster state with no dispersion of the rotators [2, 3, 7].

Notably, bicluster states are also characterized by a non-zero magnetization, with $M \sim \sqrt{e}$, where $e = E/N$ is the total energy density, with $E = H(\{\theta_i(0), p_i(0)\})$. Using the kinetic definition of the temperature $T = \langle p^2 \rangle$, this entails an anomalous energy-temperature relation, with respect to the expected equilibrium linear relation $T = 2e$ [2, 7].

Remark that this phenomenon is not compatible with linear stability analysis of the Vlasov equation [1, 3][1], which predicts the homogeneous states to be stable for all energies, for a wide class of initial distributions of momenta.

The class of initial conditions leading to a bicluster is yet not precisely known. Let $\gamma_0 = V_0/E$, with $V_0 = V(\{\theta_i(0)\})$. Previous studies [8] have shown that, at a given energy, for initially uniformly random distributions of angles and momenta (i.e. waterbag distributions, defined later in Sec. 4), the closer we are to $\gamma_0 = 1$, the more likely is the formation of the bicluster, and the larger is the stationary value of M_2. We chose to use this ratio as a control parameter for our simulations in section 4.
Nevertheless, it is worth noting that biclusters can also arise from sinusoidal initial distributions of momenta (i.e. $p_i(0) \propto \sin(\theta_i(0))$), in which case the parameter γ_0 becomes irrelevant [8]. In the present work, we will solely focus on waterbag initial distributions.

Previously, a theory has been devised to explain the formation and stabilization of a bicluster, as the equilibrium state of an averaged Hamiltonian [3], derived by using a variational method inspired by Ref. [18]. The authors of Ref. [3], separating fast and slow variables in the Lagrangian, notably predicted the occurrence of two collective high frequencies $\omega_\pm$, and gave accurate quantitative results.

In the following, we propose a new approach, to get a better understanding of the dynamical mechanism at the base of the bicluster formation and stabilization. We derive the same high frequencies $\omega_\pm$ in section 2, by directly studying the dynamics of the magnetization vector, which is the driving force of the system (see

[1] In Ref. [1], linear stability analysis was performed for the ferromagnetic model. Stability in the antiferromagnetic case can be retrieved by a simple change of sign.

Eq. (3)). This allows us, in section 3, to rewrite the equations of motions in a non-autonomous form, and thereby perform an averaging over the fast variables in a very simple fashion. An expression for the effective force is found, with associated low frequency ω_0, and its dependence to initial conditions is discussed.
Section 4 exposes our numerical results, showing excellent agreement with the theory.
In section 5, we discuss our results and develop a heuristic argument to explain the birth and stabilization of the bicluster states. We conclude by mentioning possible analogies with other models, and proposing further developments.

2. Dynamics of the total magnetization

We are interested in deriving a dynamical equation for the macroscopic quantity $\boldsymbol{M}$. We are considering here the low energy regime, for which biclusters are known to occur. From Eq. (2), we get

$$\frac{d^2}{dt^2}\boldsymbol{M}(t) = \frac{1}{N}\sum_{j=1}^{N}\begin{pmatrix} -\dot{p}_j \sin(\theta_j) - p_j^2 \cos(\theta_j) \\ \dot{p}_j \cos(\theta_j) - p_j^2 \sin(\theta_j) \end{pmatrix} . \tag{5}$$

We identify in this expression the correlator $\langle p^2 \cos(\theta)\rangle \sim o(MT) \sim o(e^{3/2})$, that we can neglect in the low energy regime, since the other term turns out to be of order $o(M) \sim o(e^{1/2})$. We are left with

$$\frac{d^2}{dt^2}\boldsymbol{M}(t) \approx \frac{1}{N}\sum_{j=1}^{N}\begin{pmatrix} -\dot{p}_j \sin(\theta_j) \\ \dot{p}_j \cos(\theta_j) \end{pmatrix} . \tag{6}$$

Then, inserting the equations of motion (3), we obtain the eigenproblem

$$\frac{d^2}{dt^2}\begin{pmatrix} M_x(t) \\ M_y(t) \end{pmatrix} \approx \begin{pmatrix} -\frac{1-M_x^{(2)}}{2} & \frac{M_y^{(2)}}{2} \\ \frac{M_y^{(2)}}{2} & -\frac{1+M_x^{(2)}}{2} \end{pmatrix}\begin{pmatrix} M_x(t) \\ M_y(t) \end{pmatrix} . \tag{7}$$

The eigenvalues and corresponding eigenvectors result

$$-\omega_\pm^2 = -\frac{1 \pm M_2}{2} \tag{8}$$

$$\boldsymbol{M_-} = \begin{pmatrix} \cos(\phi_2/2) \\ \sin(\phi_2/2) \end{pmatrix}, \quad \boldsymbol{M_+} = \begin{pmatrix} -\sin(\phi_2/2) \\ \cos(\phi_2/2) \end{pmatrix} , \tag{9}$$

where ϕ_2 is defined as the phase of $\boldsymbol{M_2}$. We hence expect the system to globally rotate with $\phi_2/2$, which already stresses the importance of $\boldsymbol{M_2}$ in the characterization of the dynamics.
Let us emphasize the consistency of this result with that one of Ref. [3], in which the modes $\omega_\pm$ were found to be the eigenvalues of the fast Lagrangian, and where $\phi_2/2$ was already recognized as the system's center of mass. These frequencies, arising from nonlinear mode interaction, can be seen as a splitting of the single normal mode $\omega = 1/\sqrt{2}$, present in the homogeneous state [8]. This normal mode can also be found by linear analysis of the Vlasov equation [3].

Assuming $\boldsymbol{M_2}$ constant, after a global rotation of $-\phi_2/2$, we get

$$\boldsymbol{M} = \begin{pmatrix} M_- \cos(\omega_- t + \phi_-) \\ M_+ \cos(\omega_+ t + \phi_+) \end{pmatrix} , \tag{10}$$

where $\phi_\pm$ are arbitrary constant phases. It is worth remarking that, in the ferromagnetic case, the eigenvalues read $\lambda_\pm \approx \frac{1 \pm M_2}{2}$, and under the same low energy hypothesis, $\boldsymbol{M}$ will rather converge to a constant, following a slow drift motion [2].

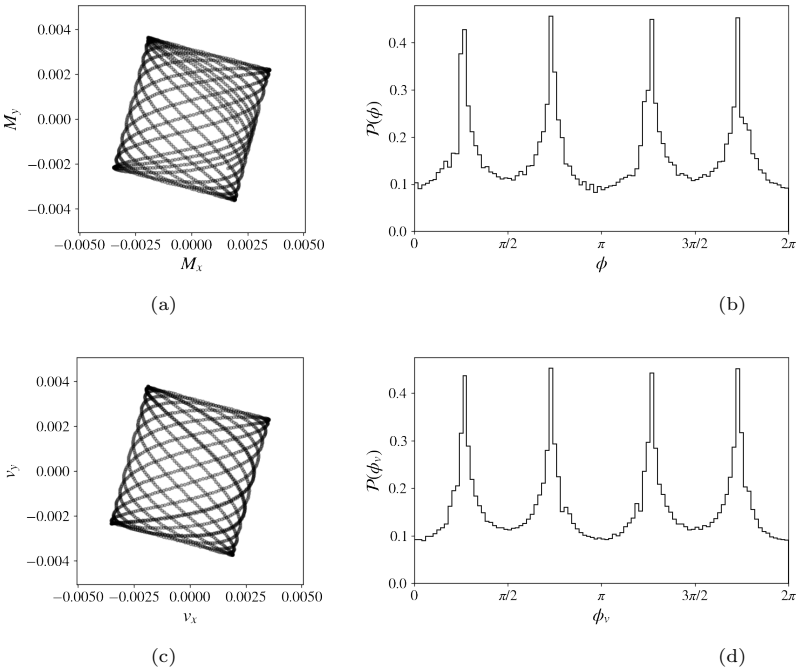

Figure 1: The dynamics and histogram of ϕ, the phase of $\boldsymbol{M}$, measured in a simulation with $\gamma_0 = 1$, $M_2 = 0.52$ (see Sec. 4, Fig. 3a). We define a vector $\boldsymbol{v}$ according to Eq. (10). The frequencies $\omega_\pm$ are drawn from measurements of M_2, the amplitudes $v_{-,+}$ respectively defined through $\max(M_{x,y})$ (after $\boldsymbol{M}$ was rotated of $-\phi_2/2$), and we finally rotate $\boldsymbol{v}$ of $\phi_2/2$, as suggested by Eq. (9). We show in Cartesian coordinates the dynamic, measured over the time interval $t \in [10000, 10100]$, of $\boldsymbol{M}$ (resp. $\boldsymbol{v}$) in Fig. 1a (resp. c). The corresponding distributions $\mathcal{P}(\phi)$ (resp. $\mathcal{P}(\phi_v)$) are reported in Fig. 1b (resp. d). Histograms are derived from a sample of values retrieved in the time interval $t \in [10000, 11000]$. We used the time step $\Delta t = 0.05$.

Fig. 1 shows the behaviour of $\boldsymbol{M}$ measured by numerical integration of the full equations of motion (3), and the one of a vector $\boldsymbol{v}$ defined according to Eq. (10). Namely, $\boldsymbol{v} = \big(v_- \cos(\omega_- t), v_+ \cos(\omega_+ t)\big)$, where $\omega_\pm$ are computed from the average value of M_2 and $v_\pm$ are measured by taking the maximum value of $M_{x,y}$, after a rotation of $-\phi_2/2$. Also, we present later, in Fig. 2a the frequency spectrum of the components M_x, M_y, derived by a fast Fourier transform, also performed after a rotation of $-\phi_2/2$. Better agreement is found for well-formed biclusters ($M_2 \gtrsim 0.1$), as we will discuss in section 4. A few other examples are displayed in Appendix A.

The parametric curves defined by Eq. (10) are named Lissajous curves. Such curves are bounded in the

(M_x, M_y)-plane by a rectangle of sides M_- and M_+, and are known to densely fill its area, provided that the ratio ω_-/ω_+ is irrational, condition that is almost always fulfilled. The norm M evidently possesses four maxima, each located at a fixed angular position. One can see from Eq. (10) that $\dot{\boldsymbol{M}}$ approaches 0 as $\boldsymbol{M}$ approaches $(\pm M_-, \pm M_+)$ (when M is maximal), making these regions favoured in terms of the amount of time spent there by the system, as illustrated in Fig. 1b.
Note that, when $M_2 \approx 0$, the curve is an ellipse, hence $\boldsymbol{M}$ exhibits two maxima. This is also the case when $M_- \ll M_+$ (or $M_- \gg M_+$). The probability density function for $\boldsymbol{M}$ is hence bimodal (at least during a first transient phase) or quadrimodal, in the considered low energy regime.

This simple derivation already provides us with a heuristic explanation for the occurrence of a bimodal distribution of the rotators in the antiferromagnetic HMF model. Indeed, as we will show below, if the rotators are slow enough with respect to $\omega_\pm$, they effectively experience a bimodal potential.
It is fairly obvious from Fig. 1 that, as this regime persists for very long times, it brings on a breaking of ergodicity. Indeed, the accessible state space is bounded by the Lissajous curve, entailing a probability density $\mathcal{P}(\phi, M)$ anomalous with respect to the expected one from equilibrium statistics. In particular, while the time average of $\boldsymbol{M}$ is null, the one of M is not. These coherent oscillations hence allow for a non-vanishing (extensive) average potential energy.

3. Time scale separation

We found above an explicit time dependence for the bare potential. By doing this, we also decoupled it from the generalized coordinates $\{\theta_j\}$. This allows us to fully take advantage of the mean-field nature of the model, hence to actually consider single rotators as uncoupled pendula, evolving under the action of an external potential driven by the oscillating "magnetic field" $\boldsymbol{M}$.

We first insert Eq. (10) in Eq.(3), thus

$$\dot{p}_j(t) = \epsilon a_- \cos(\omega_- t + \phi_-) \sin(\theta_j) - \epsilon a_+ \cos(\omega_+ t + \phi_+) \cos(\theta_j), \tag{11}$$

with $\epsilon a_\pm = M_\pm$, so that we have $a_+^2 + a_-^2 = 1$, and $\epsilon = \sqrt{M_+^2 + M_-^2} \sim \sqrt{e}$.

We are now able to perform a simple approximation, related to the *ponderomotive effect*, well-known in the area of plasma physics [19]. As the one employed in Ref. [3], it relies on the clear separation of time scales between fast and slow variables, and is somehow analogous to the method first proposed by Landau and Lifshitz to solve systems exhibiting two distinct time scales [20]. The prototypical example of such systems is the Kapitza pendulum [21].

Our use of this approximation method is justified by the consideration that, already in Eq. (11), one can clearly identify the two time scales of the motion. The first is a fast one, related to the motion of the phase, which is set by the frequencies $\omega_\pm \sim 1$. The second is a slow one, and is proportional to the square root of

the amplitude of the acceleration, giving a time scale of the order $\sqrt{\epsilon}$, which in fact characterizes the motion of a pendulum at the bottom of the potential.

Let us decompose the variables in a fast and a slow component. We set the magnitude of the fast component to be $o(\epsilon)$, and introduce a "slow time" $\tau = \epsilon t$, associated to the slow oscillations, insuring $\langle \dot{p}_j^2 \rangle \sim \epsilon^2$,

$$\theta_j(t) = \theta_j^0(\tau, t) + \epsilon f_j(t)\,. \tag{12}$$

The single rotator dynamics thus presents a fast motion of small amplitude, superimposed with a slow motion of large amplitude.

Expanding Eq. (11) up to first order in ϵf_j, we obtain

$$\begin{aligned}\epsilon^2 \frac{d^2}{d\tau^2}\theta_j^0(\tau,t) + \epsilon \frac{d^2}{dt^2} f_j(t) =& \epsilon\Big(a_- \cos(\omega_- t + \phi_-)\sin(\theta_j^0(\tau)) - a_+ \cos(\omega_+ t + \phi_+)\cos(\theta_j^0(\tau))\Big) \\ &+ \epsilon^2 f_j(t)\Big(a_- \cos(\omega_- t + \phi_-)\cos(\theta_j^0(\tau)) + a_+ \cos(\omega_+ t + \phi_+)\sin(\theta_j^0(\tau))\Big)\,.\end{aligned} \tag{13}$$

By identifying terms order by order, we get the following expression for the fast variables

$$\frac{d^2}{dt^2} f_j(t) = a_- \cos(\omega_- t + \phi_-)\sin(\theta_j^0(\tau)) - a_+ \cos(\omega_+ t + \phi_+)\cos(\theta_j^0(\tau))\ , \tag{14}$$

which we can straightforwardly integrate, since $\theta_j^0(\tau)$ is considered constant on the time scale of $f_j(t)$. It results

$$f_j(t) = -\frac{a_-}{\omega_-^2}\cos(\omega_- t + \phi_-)\sin(\theta_j^0(\tau)) + \frac{a_+}{\omega_+^2}\cos(\omega_+ t + \phi_+)\cos(\theta_j^0(\tau))\,. \tag{15}$$

Then, by substituting this expression for $f_j(t)$ in Eq. (13), we obtain after some manipulations (for convenience, we dropped the time dependence and the constant phases $\phi_\pm$)

$$\begin{aligned}\frac{d^2}{dt^2}\theta_j^0 =& \frac{1}{4}\left[\frac{M_+^2}{\omega_+^2}\Big(1+\cos(2\omega_+ t)\Big) - \frac{M_-^2}{\omega_-^2}\Big(1+\cos(2\omega_- t)\Big)\right]\sin(2\theta_j^0) \\ &+ \frac{1}{4}\left[\frac{M_+M_-}{\omega_+^2}\Big(1+\cos(2\theta_j^0)\Big) - \frac{M_+M_-}{\omega_-^2}\Big(1-\cos(2\theta_j^0)\Big)\right]\Big(\cos((\omega_- + \omega_+)t) + \cos((\omega_- - \omega_+)t)\Big)\,.\end{aligned} \tag{16}$$

If M_2 is of the order of ϵ then $(\omega_+ - \omega_-)$ is of the order of ϵ, a low frequency that cannot be neglected by averaging over the fast oscillations. Then, our computation holds when $M_2 \gg \epsilon$, and a priori does not account for the beginning of the transient. By averaging over the fast oscillations, we get the expression for the slow variables

$$\frac{d^2}{dt^2}\theta_j^0 \approx \frac{1}{4}\Big(\frac{M_+^2}{\omega_+^2} - \frac{M_-^2}{\omega_-^2}\Big)\sin(2\theta_j^0)\,. \tag{17}$$

Assuming that the prefactor is negative, we can consider a rotator in the bottom of one potential well, located at $\theta_j^0 \approx k\pi$, with $k \in \mathbb{Z}$, so $\sin(2\theta_j^0) \approx 2\theta_j^0 - 2k\pi$. We then have

$$\theta_j^0(t) \approx k\pi + A_j \cos(\omega_0 t + \phi_j),\ \text{with} \tag{18}$$

$$\omega_0 = \frac{1}{\sqrt{2}}\sqrt{\frac{M_-^2}{\omega_-^2} - \frac{M_+^2}{\omega_+^2}}\,. \tag{19}$$

ω_0 is of the order of M, namely the square of the natural frequency. This emphasizes that the effective force emerges from the non-linearity, linked to the self-consistency of the magnetization.

The attractive or repulsive nature of this bimodal effective interaction, is related to the sign of the prefactor in Eq. (17), namely

$$\Delta - M_2 < 0 \ , \tag{20}$$

with $\Delta = \frac{M_+^2 - M_-^2}{M_+^2 + M_-^2}$. The effective force is self-consistent, in the sense that its strength is proportional to M_2, which is governed by the force itself. Thus, we are brought to assume that M_+, M_- and M_2 are evolving during a transient phase in an interdependent fashion, following a dynamics which is determined by the initial conditions. In particular, we will comment in next section, based on numerical observations, that the bicluster forms when the initial condition is a waterbag such that $\gamma_0 \sim 1$.

This result provides a dynamical explanation for the stabilization of biclusters over very long times.

4. Numerical results

Our simulations were performed at energies ranging from 10^{-5} to 10^{-4}, with $N = 1000$. The equations of motions have been integrated using a fourth-order sympleptic scheme [22]. For most of the figures, we used a time step $\Delta t = 0.05$, which gives a conservation of the energy up to $\Delta e \sim 10^{-12}$. On the contrary, to produce Fig. 5, we used a more efficient time step $\Delta t = 0.5$, yielding $\Delta e \sim 10^{-6}$. For the purpose of measuring a low frequency, with an efficient integrating scheme and at these ranges of energy, such a time step remains of an acceptable precision.

We initially set a water-bag distribution, picking the positions and momenta uniformly at random in a domain $[-\pi, \pi] \times [-p_0, p_0]$. We used the prescription of Ref. [8] to use γ_0 as a control parameter. To do this, we first find, by iterating multiple times, a distribution of positions giving a potential energy in the desired range. Then we choose p_0 to set $T = \langle \dot{\theta_j}^2 \rangle$ accordingly, and globally shift the momenta to set the constant of motion $\langle p_j \rangle = 0$.

The averages are taken after a transient, typically of the order of 10000 proper times. We have checked that the averages do not change by increasing the duration of the transient. By looking directly at the time series, we have also checked that the system has reached a steady state after the transient.

In the literature [2, 3, 7], as well as in our own simulations, the parameter M_2 has never been reported to exceed 0.8.

In Fig. 2 is shown an example of the short term dynamics of $\boldsymbol{M}$, along with the corresponding Fourier spectra of its components, performed after a global rotation of $-\phi_2/2$. Here, the agreement of experimental data with Eq. (10) is excellent.

For small M_2, the agreement of $\boldsymbol{M}$ with Eq. (10) is not as good. Though collective oscillations still occur,

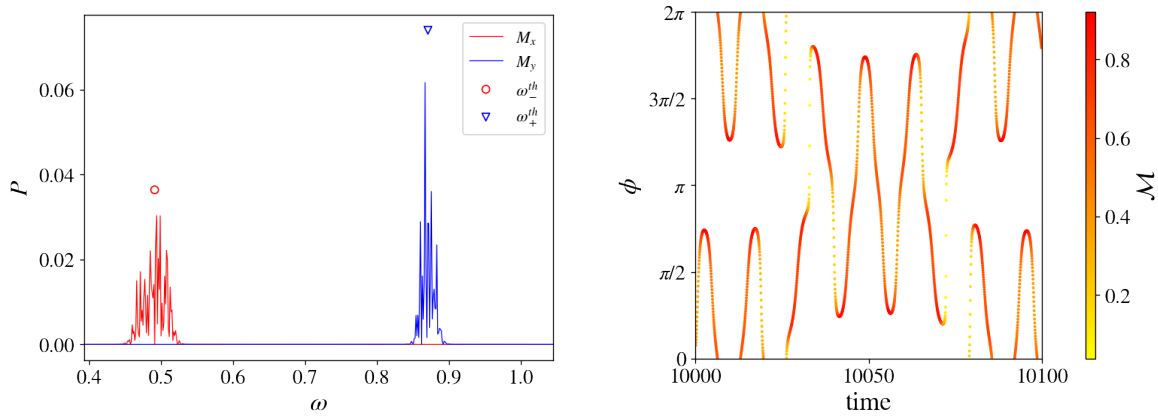

(a) Frequency spectrum of M_x and M_y.

(b) Short time phase trajectory of $\boldsymbol{M}$.

Figure 2: Power spectrum and detail of the trajectory of $\boldsymbol{M}$, with $\gamma_0 = 1$, $M2 = 0.52$, $\Delta = -0.09$ (see Fig. 3a).

the envelopes $M_\pm$ fluctuate, and the trajectories of the magnetization lose their regularity. However, we observed the fast collective oscillations to be present from the beginning, regardless of the later formation of a bicluster (hence of the value of γ_0), and before the system has reached a steady state. The average value of $\mathcal{M} = M/\sqrt{2e}$ is related to γ_0: a high initial value leads to an accordingly high average of $\langle \mathcal{M} \rangle$.

Fig. 3 shows the general dynamics of the system, at different values of the parameters. Here, the existence of two distinct time scales is manifest: the one associated to the fast oscillation of $\boldsymbol{M}$, is visibly much smaller than the one associated to the long-term behaviour of the single rotator dynamics. In this view, it is evident that the dynamics associated to the slow variables is similar to one of a rotator in a bimodal potential. Indeed, we can clearly see two angular regions "favoured" by $\boldsymbol{M}$ in terms of the time spent as well as in magnitude. These are the locations of the two clusters, following as expected the same slow linear drift as $\phi_2/2$. Around these regions some trapped rotators (below the separatrix) slowly oscillate, while some untrapped ones (above the separatrix) are evolving in an almost ballistic fashion.

Note that well-formed biclusters seem to occur regardless of the value of Δ. Indeed, we were not able to find a clear relation of the stationary value of Δ neither with γ_0 nor with the stationary value of M_2. Although we have found that the effective force Eq. (17) can become very slightly repulsive when $\gamma_0 \approx 0$, it ends up attractive in the vast majority of cases. Also, Δ and M_2 evolve, at a slow time scale with respect with $\omega_\pm$, towards values satisfying Eq. (20).

To investigate the spectral properties of the rotator trajectories, we focused on initial conditions leading to sufficiently well-formed biclusters, i.e. $M_2 \gtrsim 0.2$ ($\gamma_0 > 0.7$), and performed the global rotation of $-\phi_2/2$ to follow the center of mass.

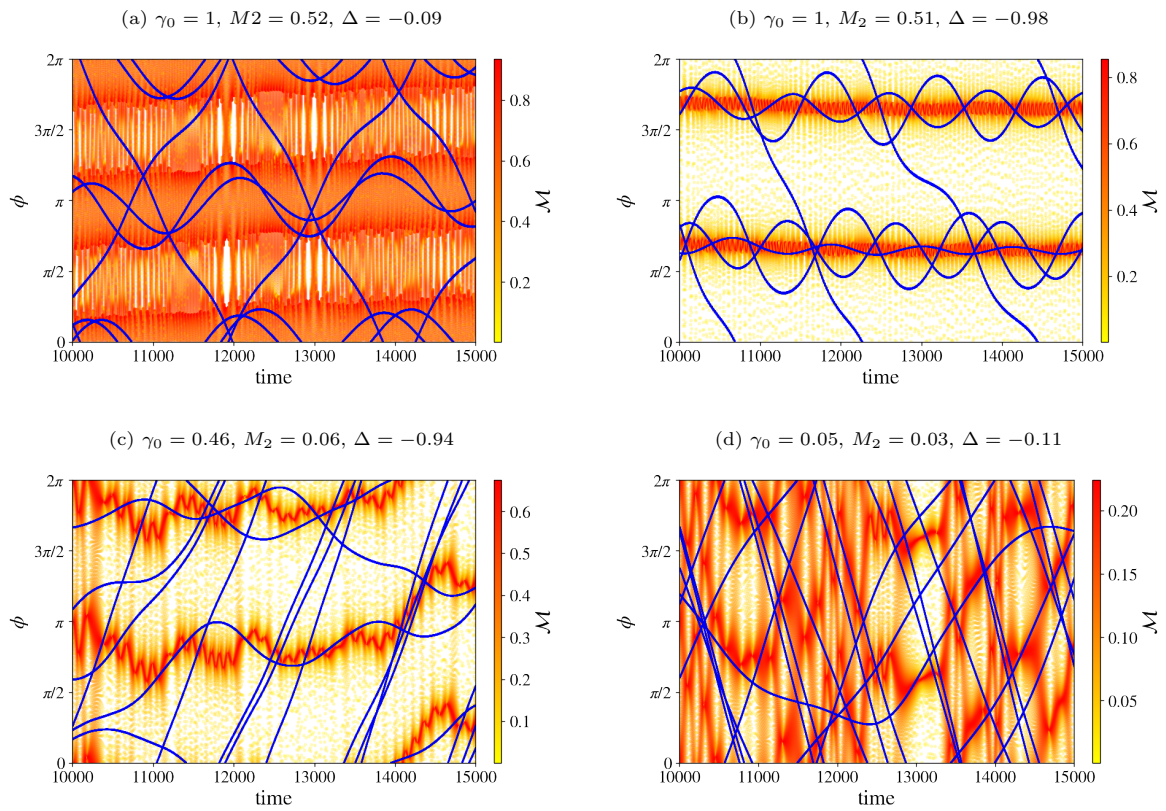

Figure 3: Some rotators trajectories are shown in blue, along with the magnetization in a red gradient; the color gradient indicates the rescaled norm $\mathcal{M} = M/\sqrt{2e}$. Energy was set to $e \sim 10^{-5}$.

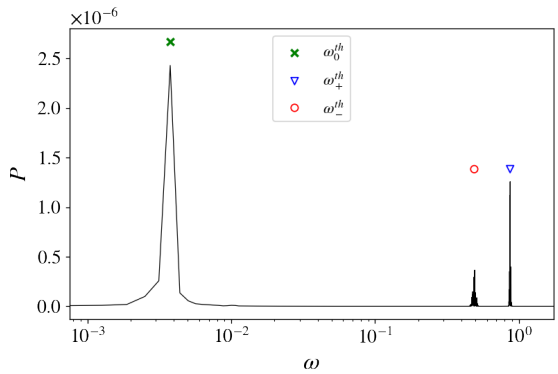

Figure 4: Power spectrum of a single trapped rotator from figure 3a.

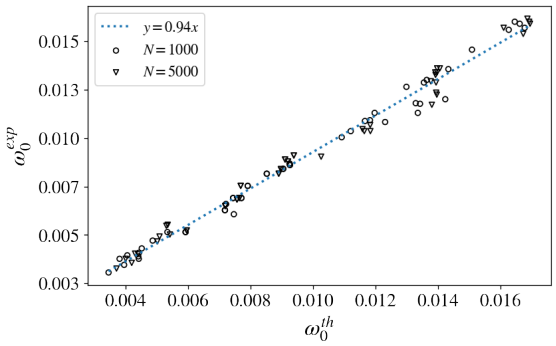

Figure 5: Comparison of ω_0 theoretical and experimental. We performed Fourier transforms on small random subsets of trapped rotators, at energies ranging from 10^{-5} to 10^{-4}.

Fig. 4 shows an example of a single rotator Fourier spectrum, trapped in a potential well and oscillating with a small amplitude. The slow mode ω_0 is not present in the spectra of the untrapped rotators, or is very weak and with a higher discrepancy with Eq. (19).

In the considered regime, the low frequency observed in simulations agrees with our theoretical value,

up to a multiplicative factor of order 1, namely $\omega_0^{exp} \approx 0.94\omega_0^{th}$, as shown in Fig. 5.

5. Conclusions and perspectives

In the light shed by these results, let us synthesize and propose a scenario accounting for the formation of biclusters in the antiferromagnetic HMF model, from a waterbag initial distribution.

At low energy, an initial state of small but non-vanishing magnetization generates a collective oscillatory regime. This is due to the self-consistency of $\boldsymbol{M}$, which repels all of the rotators, entailing its own motion towards the opposite angle, in a periodic fashion. The time scale associated to this collective motion is much smaller than the typical time scale of the individual rotators. We observe a cyclic high frequency transfer of energy between kinetic and potential, and the system periodically returns close to its initial high value of the $\gamma = M^2/2E$ ratio. This entails the non-vanishing $\langle M \rangle$. If, initially, the temperature is small with respect to the potential energy, the magnetization vector $\boldsymbol{M}$ follows a Lissajous-type regular curve parametrized by $\omega_\pm = \sqrt{\frac{1-M_2}{2}}$ and $M_\pm$, as described in Eq. (10). The phase of $\boldsymbol{M}$ is rapidly oscillating between two or four symmetric angles, and we thus have $\langle \boldsymbol{M} \rangle = \boldsymbol{0}$ and, near one of the maxima, rotators are subjected to repulsive and attractive forces, alternatively.
In the very beginning, as $M_2 \approx 0$, $\omega_- \approx \omega_+ \approx 1/\sqrt{2}$, and $\boldsymbol{M}$ follows an almost elliptic trajectory, and thus exhibits two maxima in magnitude at two opposite angular positions. The variables $\omega_\pm$, $M_\pm$, are evolving concomitantly with M_2, at a slow rate. As M_2 increases, the unique frequency of $\boldsymbol{M}$ split into two, and the two maxima (generally) split into four.
When the difference between the two frequencies becomes large enough, a bimodal effective force can be derived, accounting for the stabilization of the bicluster.

The nature of this effective force is determined by Eq. (20). A full understanding of the conditions leading to a stable bicluster would thus involve a thorough study of the transient dynamics of the slow macroscopic variables $\boldsymbol{M_2}$, M_+ and M_-.
It would also require to explain how other types of initial distributions (in particular, initial sinusoidal distributions of momenta, with vanishing initial magnetization) relate to the processes described above.

The study of the dynamics of this simple mean-field model provides valuable insights into the mechanisms leading to ergodicity breaking in long-range interacting systems.
We have stressed the importance of the self-consistency of the potential, giving rise to nonlinear effects, solvable through multiscale analysis. This self-consistency is characteristic of mean-field models; an interesting development would hence be to look for the presence of biclusters and collective oscillations in modified versions of the antiferromagnetic HMF, weakening this self-consistency. This emergent behaviour has been shown to be preserved in presence of a nearest-neighbour ferromagnetic or antiferromagnetic perturbative interaction [13]; the phenomenon is hence not specific of pure mean-field models.

In recent studies, it has been noticed that the HMF model presents strong similarities with systems of cold atoms in optical cavities [23, 24]. Such systems can be considered as almost isolated, thus opening the possibility of performing a "real-life experiment" showing the non-trivial ordered phases discussed in this paper.

Acknowledgments R.F. acknowledges support by the QuantERA ERA-NET Co-fund 731473 (Project Q-CLOCKS). S.R. is financially supported by the MISTI Global Seed Funds MIT-FVG Collaboration Grant "NV centers for the test of the Quantum Jarzynski Equality (NVQJE)", and the MIUR-PRIN2017 project "Coarse-grained description for non-equilibrium systems and transport phenomena (CO-NEST)" No. 201798CZL.

Appendix A. Examples of magnetization dynamics

Below are shown the dynamics of $\boldsymbol{M}$ in Cartesian coordinates, along with the corresponding distributions $\mathcal{P}(\phi)$, from different simulations. The histograms are derived from samples of values retrieved in the time interval $t \in [10000, 11000]$, while the dynamics are bounded by the time interval $t \in [10000, 10100]$. We used the time step $\Delta t = 0.05$.

The upper figures display the dynamics directly retrieved from simulations, while the lower ones shows the same views of a vector $\boldsymbol{v}$ defined using Eq. (10). The frequencies $\omega_\pm$ are drawn from measurements of M_2, $v_\pm = \max(M_{x,y})$ (with $\boldsymbol{M}$ rotated of $-\phi_2/2$), and we finally rotate $\boldsymbol{v}$ of $\phi_2/2$, as suggested by Eq. (9).

Visibly, the discrepancy between the real dynamics and our analytical formula is higher for less well-formed biclusters. This is due to the fact that, as mentioned is section 4, in this regime, the amplitudes $M_\pm$ are fluctuating, whereas our parameters $v_\pm$ are constant.

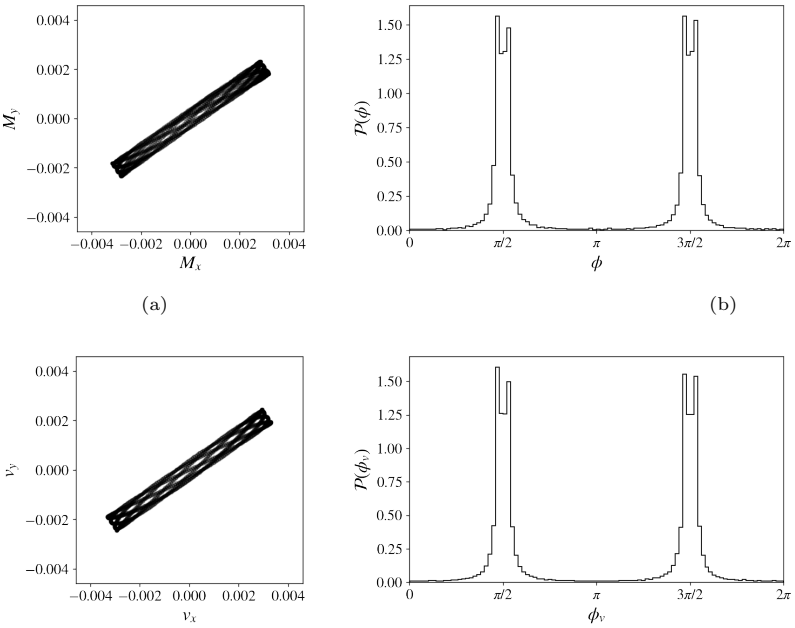

Figure A.6: $\gamma_0 = 1$, $M_2 = 0.51$, $\Delta = -0.98$, long-time behaviour shown in Fig. 3b

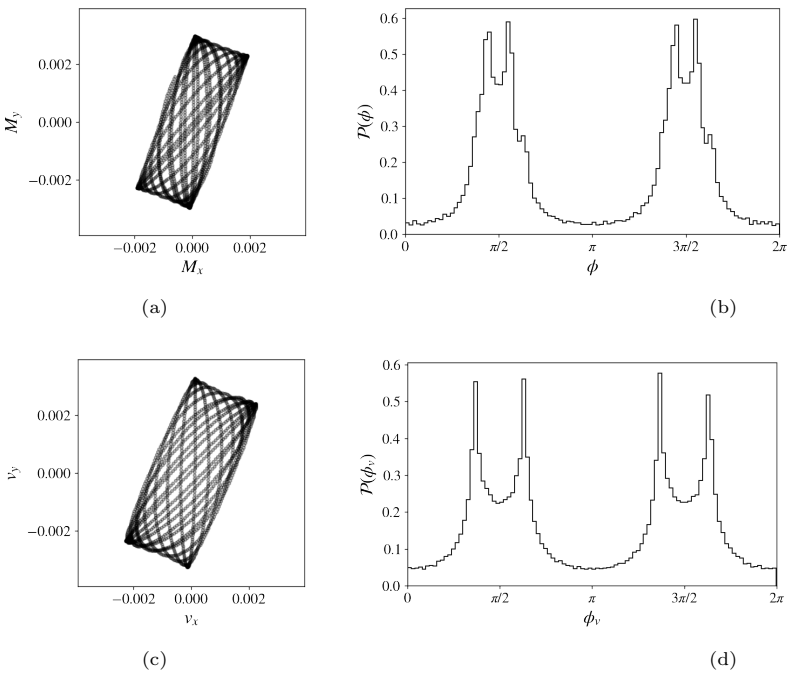

Figure A.7: $\gamma_0 = 0.46$, $M_2 = 0.06$, $\Delta = -0.94$, long-time behaviour shown in Fig. 3c

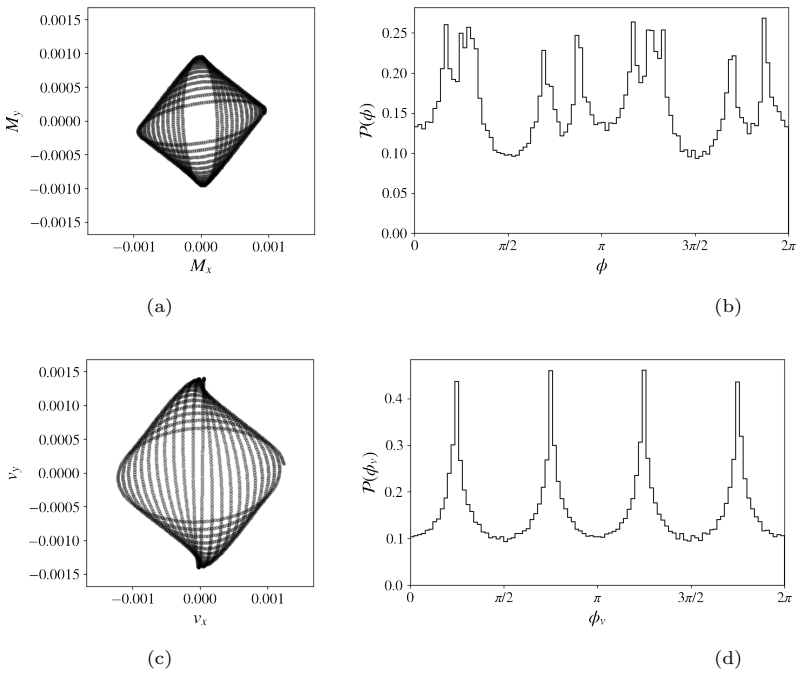

Figure A.8: $\gamma_0 = 0.05$, $M_2 = 0.03$, $\Delta = -0.11$, long-time behaviour shown in Fig. 3d

References

[1] A. Campa, T. Dauxois, S. Ruffo, Statistical mechanics and dynamics of solvable models with long-range interactions, Physics Reports 480 (3-6) (2009) 66–68, arXiv: 0907.0323. doi:10.1016/j.physrep.2009.07.001.
URL http://arxiv.org/abs/0907.0323

[2] M. Antoni, S. Ruffo, Clustering and relaxation in Hamiltonian long-range dynamics, Physical Review E 52 (3) (1995) 2361–2374. doi:10.1103/PhysRevE.52.2361.
URL https://link.aps.org/doi/10.1103/PhysRevE.52.2361

[3] J. Barre, F. Bouchet, T. Dauxois, S. Ruffo, Birth and long-time stabilization of out-of-equilibrium coherent structures, The European Physical Journal B - Condensed Matter 29 (4) (2002) 577–591, arXiv: cond-mat/0203013. doi:10.1140/epjb/e2002-00342-3.
URL http://arxiv.org/abs/cond-mat/0203013

[4] J. Barré, F. Bouchet, T. Dauxois, S. Ruffo, Out-of-Equilibrium States as Statistical Equilibria of an Effective Dynamics in a System with Long-Range Interactions, Physical Review Letters 89 (11) (2002) 110601. doi:10.1103/PhysRevLett.89.110601.
URL https://link.aps.org/doi/10.1103/PhysRevLett.89.110601

[5] A. Campa, A. Giansanti, D. Mukamel, S. Ruffo, Dynamics and thermodynamics of rotators interacting with both long- and short-range couplings, Physica A: Statistical Mechanics and its Applications 365 (1) (2006) 120–127. doi:10.1016/j.physa.2006.01.003.
URL https://linkinghub.elsevier.com/retrieve/pii/S0378437106000446

[6] T. Dauxois, V. Latora, A. Rapisarda, S. Ruffo, A. Torcini, The Hamiltonian Mean Field Model: from Dynamics to Statistical Mechanics and back, arXiv:cond-mat/0208456ArXiv: cond-mat/0208456 (Aug. 2002).
URL http://arxiv.org/abs/cond-mat/0208456

[7] T. Dauxois, P. Holdsworth, S. Ruffo, Violation of ensemble equivalence in the antiferromagnetic mean-field XY model, The European Physical Journal B 16 (4) (2000) 659–667. doi:10.1007/s100510070183.
URL http://link.springer.com/10.1007/s100510070183

[8] D. Jeong, J. Choi, M. Y. Choi, Collective oscillations, bicluster motion, and dynamical order in a system of globally coupled rotors with repulsive interactions, Physical Review. E, Statistical, Nonlinear, and Soft Matter Physics 74 (5 Pt 2) (2006) 056106. doi:10.1103/PhysRevE.74.056106.

[9] X. Leoncini, T. L. V. D. Berg, D. Fanelli, Out of Equilibrium Solutions in the XY-Hamiltonian Mean Field model, EPL (Europhysics Letters) 86 (2) (2009) 20002, arXiv: 0809.3709. doi:10.1209/0295-5075/86/20002.
URL http://arxiv.org/abs/0809.3709

[10] Y. Y. Yamaguchi, J. Barr'e, F. Bouchet, T. Dauxois, S. Ruffo, Stability criteria of the Vlasov equation and quasi-stationary states of the HMF model, Physica A: Statistical Mechanics and its Applications 337 (1-2) (2004) 36–66, arXiv: cond-mat/0312480. doi:10.1016/j.physa.2004.01.041.
URL http://arxiv.org/abs/cond-mat/0312480

[11] J. Dawson, One-Dimensional Plasma Model, The Physics of Fluids 5 (4) (1962) 445–459, _eprint: https://aip.scitation.org/doi/pdf/10.1063/1.1706638. doi:10.1063/1.1706638.
URL https://aip.scitation.org/doi/abs/10.1063/1.1706638

[12] O. C. Eldridge, M. Feix, One-Dimensional Plasma Model at Thermodynamic Equilibrium, The Physics of Fluids 5 (9) (1962) 1076–1080, _eprint: https://aip.scitation.org/doi/pdf/10.1063/1.1724476. doi:10.1063/1.1724476.
URL https://aip.scitation.org/doi/abs/10.1063/1.1724476

[13] A. Vesperini, Dynamics and thermodynamics of the HMF model with additional short-range interactions, Master thesis, SISSA, Trieste (Jun. 2020).

[14] X. Leoncini, Self-organized regularity in long-range systems, in: E. Ugalde, H. Gonzales-Aguilar (Eds.), Nonlinear Dynamics New Directions, Vol. 12 of Nonlinear Systems and Complexity, Springer, 2015, pp. 79–109. doi:10.1007/978-3-319-09864-7.
URL https://hal.archives-ouvertes.fr/hal-01275889

[15] A. Turchi, D. Fanelli, X. Leoncini, Emergence of a collective crystal in a classical system with long-range interactions, EPL (Europhysics Letters) 111 (3) (2015) 30011. doi:10.1209/0295-5075/111/30011.
URL https://iopscience.iop.org/article/10.1209/0295-5075/111/30011

[16] S. De Nigris, X. Leoncini, Emergence of a non trivial fluctuating phase in the XY model on regular networks, EPL (Europhysics Letters) 101 (1) (2013) 10002, arXiv: 1207.6550. doi:10.1209/0295-5075/101/10002.
URL http://arxiv.org/abs/1207.6550

[17] R. Plestid, P. Mahon, D. O'Dell, Violent relaxation in quantum fluids with long-range interactions, Physical Review E 98 (1) (2018) 012112, arXiv: 1610.01582. doi:10.1103/PhysRevE.98.012112.
URL http://arxiv.org/abs/1610.01582

[18] G. B. Whitham, Linear and Nonlinear Waves, John Wiley & Sons, 2011.

[19] G. Schmidt, II - Motion of Charged Particles in Electromagnetic Fields, in: G. Schmidt (Ed.), Physics of High Temperature Plasmas (Second Edition), second edition Edition, Academic Press, 1979, pp. 5–54. doi:10.1016/B978-0-12-626660-3.50006-7.
URL https://www.sciencedirect.com/science/article/pii/B9780126266603500067

[20] L. D. Landau, E. M. Lifshitz, Chapter V - Small oscillations, in: L. D. Landau, E. M. Lifshitz (Eds.), Mechanics (Third Edition), third edition Edition, Butterworth-Heinemann, Oxford, 1976, pp. 58–95. doi:10.1016/B978-0-08-050347-9.50010-1.
URL https://www.sciencedirect.com/science/article/pii/B9780080503479500101

[21] P. Kapitza, Collected Papers of PL Kapitza, edited by D. ter Haar Pergamon, Oxford 1941 (1965) 714, 726.
[22] R. I. McLachlan, P. Atela, The accuracy of symplectic integrators, Nonlinearity 5 (2) (1992) 541–562, publisher: IOP Publishing. doi:10.1088/0951-7715/5/2/011.
URL https://doi.org/10.1088/0951-7715/5/2/011
[23] S. Schütz, S. B. Jäger, G. Morigi, Dissipation-assisted prethermalization in long-range interacting atomic ensembles, Physical Review Letters 117 (8) (2016) 083001, arXiv: 1512.05243. doi:10.1103/PhysRevLett.117.083001.
URL http://arxiv.org/abs/1512.05243
[24] S. Schütz, G. Morigi, Prethermalization of Atoms Due to Photon-Mediated Long-Range Interactions, Physical Review Letters 113 (20) (2014) 203002. doi:10.1103/PhysRevLett.113.203002.
URL https://link.aps.org/doi/10.1103/PhysRevLett.113.203002